Simulation of a Temporal Hard-Limited OCDMA System over FSO Link under Average Turbulence

Vítor Gouvêa Andrezo Carneiro, Gilberto Kirk Rodrigues and Maria Thereza M. Rocco Giraldi
Photonics Laboratory – Electrical Engineering Department
Instituto Militar de Engenharia
Praça General Tibúrcio, 80, Rio de Janeiro, Brazil
vitorandrezo@yahoo.com.br, kirk_ime@yahoo.com.br, mtmrocco@ime.eb.br

***Abstract*— In this paper, the feasibility and performance of a complete Optical Code Division Multiple Access system over Free Space Optics link under weak atmospheric turbulence is demonstrated through simulation. The system is proposed for multiple users sharing a single optical wireless channel to transmit coded information. It can be an initial step in mobile optical networks with multiple addressable nodes and multidirectional receivers. Usual optical sequences, such as Prime Codes, are used. The effects of variable number of users and different code lengths are considered in terms of Bit Error Rate, which is evaluated for different channel distances and divergence angles. The effects of extinction ratio in modulators, transmitter laser linewidth and carrier phase shift in delay lines are taken into account. It is shown that these effects impose a precise control of power in the hard-limiter stage.**

***Index Terms*—** Optical Code Division Multiple Access (OCDMA), Free Space Optics (FSO), Hard-Limiter, Optical Orthogonal Codes.

I. INTRODUCTION

The first developments of FSO links were dedicated to defense applications. Nowadays, these systems are recognized as important broadband access medium in next generation networks, both in commercial and military solutions [1]-[2]. FSO, also called Optical Wireless, is a re-emerging technology, which uses modulated optical focused beams to establish wireless data transmission [3]-[4].

FSO links combine high data rates (~ 2.5 Gbps in commercial solutions) with short deployment time, which allows high network reconfigurability. These characteristics, along with license-free operation and insensitivity to electromagnetic interference or jamming, make FSO systems interesting for many applications. Other advantage, derived from its confined optical beam (divergence angles from 0.05 to 10 mrad [4]), is the ability to provide significant degrees of physical security and immunity to interception.

Such links are suitable for 1 to 2 Gbps rates over distances in the range of 1 to 5 km [5]. Higher data rates and distances are possible, but under ideal conditions or using multiplexing techniques, such as dense wavelength division multiplexing (DWDM), which is yet the most common in optical systems. In terms of multiplexing, new similar works in the literature present a 1,28 Tbps DWDM system over FSO with 32 multiplexed channels, each one presenting data rates of 40 Gbps [6]-[7]. However, optical waves through the air are vulnerable to atmospheric phenomena, such as scintillation and attenuation due to fog and rain, which affect the signals, reducing the system range or requiring the use of complex modulation and coding techniques. Different

Brazilian Microwave and Optoelectronics Society-SBMO *received 18 March 2013; for review 24 Apr 2013; accepted 12 July 2013*
Brazilian Society of Electromagnetism-SBMag *ISSN 2179-1074*

modulations are employed in FSO systems but the most usual techniques are ON-OFF keying (OOK), binary phase-shift keying (BPSK) and pulse position modulation (PPM) [5].

However, most FSO systems use ON-OFF keying (OOK) with Intensity Modulation/Direct Detection (IM/DD), which is not adequate to logically hide the information, if the beam is intercepted. This scenario must be considered, especially in case of long-haul mobile system with large divergence angles.

Code Division Multiple Access (CDMA) is a spread spectrum technique that provides efficient access to the channel, by allowing many users to access it asynchronously. This access is made through the assignment of a unique signature code from a family of codes. These signatures turn the signal more difficult to be found (or read) by a possible intercepting receiver, if the codes are not known. In addition, sometimes a group of codes can be assigned to the same user, where the code is chosen dynamically. Hence, the system security can be further improved, which does not happen in access topologies other than CDMA.

The optical version of CDMA (OCDMA) is expected to aggregate the advantages of the RF version with the high bandwidth of optical medium [8]. The signature codes are usually called optical orthogonal codes (OOC) and they must satisfy certain correlation properties in order to reduce the multiple-access interference (MAI) and support various traffic demands in terms of bandwidth and BER (Bit Error Rate) performance [8]-[9].

OCDMA is currently being viewed as an alternative for usual access technologies. Since most of the traffic in network is bursty, asynchronous multiplexing schemes, like OCDMA, allow users to share the entire channel capacity dynamically and are more suitable than synchronous ones, such as wavelength division multiple access (WDMA) and optical time division multiple access (OTDMA) [10]. Modern OCDMA systems implement coherent codes, which manipulate the phase of the optical field and not only its intensity, or bidimensional codes (2D), which perform time and spectral coding simultaneously. An example of such 2D system used spectral phase-encoded time spreading (SPECTS) to achieve a capacity of 320 Gbps (32 users × 10 Gbps) [11] – [12]. Other similar work analyses the performance of SCM-FSO links for CDMA signals under strong turbulence [1].

In this paper, a complete OCDMA system over FSO link under weak atmospheric turbulence is simulated and its feasibility is demonstrated. In order to evaluate the MAI, variable number of users and different code lengths are used and the system performance is analyzed in terms of BER. This work contributes with the impact analysis of some FSO characteristics, such as different channel distances and divergence angles, over the OCDMA general system performance. In addition, more realistic effects are taken into account, such as extinction ratio in modulators, transmitter laser linewidth, carrier phase shift in delay lines and hard-limiters with non-instantaneous threshold response.

This paper is organized as follows. In Section II, optical orthogonal codes are analyzed. Section III presents detailed design concept and analysis of the OCDMA-FSO system adopted. In Section IV, the simulation parameters and numerical results are shown and discussed. Finally, the conclusions are presented in Section V.

II. OOC ANALYSIS

In this work, an incoherent OCDMA system using temporal codes is simulated. Temporal (also called Direct Sequence – DS) OCDMA uses very short optical pulses (*chips*) to perform the coding in time domain. In such systems, each bit is mapped into a very high rate sequence. The so called *chip* rate (B_c) is given by $B_c = B \times N$, where B is the bit rate and N is the code length.

Brazilian Microwave and Optoelectronics Society-SBMO *received 18 March 2013; for review 24 Apr 2013; accepted 12 July 2013*
Brazilian Society of Electromagnetism-SBMag *ISSN 2179-1074*

The performance of an OCDMA system depends on the choice of a good set of signature codes. An OOC is a binary periodic sequence of the form ($c(0)$, $c(1)$,..., $c(N\text{-}1)$) with each $c(n) \in \{0,1\}$. A set of four parameters (N, W, λ_a, λ_c) is usually adopted to characterize an OOC family, where the parameters are the code length, weight, auto- and cross-correlation constraints, respectively [8], [13]-[14].

Strict orthogonality would require that $\lambda_a = \lambda_c = 0$, but this is not possible for a unipolar system, like IM/DD, used in this work. Hence, an optical code is called strict OOC, when $\lambda_a = \lambda_c = 1$ [8]-[9], [13]-[14]. Good OOCs must maximize W and minimize λ_a and λ_c.

Let $P_{Tc}(t)$ be a rectangular pulse of duration T_c, where T_c is called the *chip* time and is $1/N$ of the bit time T_b, i.e., $T_b = NT_c$. Thus, the OOC signal of the kth user is [14]-[15]:

$$c_k(t) = \sum_{n=0}^{N-1} c_k(n) P_{Tc}(t - nT_c) \tag{1}$$

where t represents the time $\in \Re$.

Now let $s_k(t)$ be the transmitted signal of the kth user. As the modulation used is OOK and the bit rate is assumed to be the same for all users, $s_k(t)$ can be given by [16]:

$$s_k(t) = \sum_{t=-\infty}^{\infty} b_k(i) c_k(t - iT_b) \tag{2}$$

where $b_k(i) \in \{0,1\}$ is the ith bit of the kth user.

If $\tau_k \in [0,T_b)$ is the time offset of the kth user from a selected time origin, the combined transmitted signal $s(t)$ after all users are coupled together is given by [15]-[16]:

$$s(t) = \sum_{k=1}^{K} s_k(t - \tau_k) \tag{3}$$

where K is the number of users.

A. Prime Codes (PC)

Strict OOCs are highly sparse codes and the number of supported users can be very low. Hence, another important type of code, proposed for OCDMA systems, is known as prime code [10], [17]-[20]. Prime codes have higher values of λ_a compared to strict OOCs, but they can support more users and are easily generated [8]. Because of this ease of generation, they were chosen as a first proposition of mobile OCDMA network, where the FSO channel influence could be analyzed.

Prime codes have length $N = P^2$ and are derived from prime sequences of length P, obtained from a Galois field $GF(P)$, where P is a prime number [17]. A prime sequence $S_k = (s_{k0}, s_{k1},\ldots, s_{kj},\ldots, s_k(P\text{-}1))$ is evaluated by multiplying every element j of $GF(P)$ by an element k of $GF(P)$ modulo P [10]. This way, P distinct prime sequences can be obtained and transformed into a time-mapped binary code sequence $c_k(n)$, composed of P blocks of length P, each block containing a single pulse. $c_k(n)$ is given by [10], [18]-[19]:

$$c_k(n) = \begin{cases} 1, for\ n = s_{kj} + jP; s_{kj} = k \otimes j \\ 0, otherwise \end{cases} \tag{4}$$

where $j = 0, \ldots, P\text{-}1$ and $\otimes$ is the modulo P multiplication.

Brazilian Microwave and Optoelectronics Society-SBMO *received 18 March 2013; for review 24 Apr 2013; accepted 12 July 2013*
Brazilian Society of Electromagnetism-SBMag *ISSN 2179-1074*

The number of possible users in an OCDMA system using prime sequences is $K = P$ and it can be shown that PCs are sequences with ($N = P^2$, $W = P$, $\lambda_a = P$-1, $\lambda_c = 2$) [18]. The high value of λ_a makes the synchronization more difficult at the receiving end. Nevertheless, more users can be addressed using prime codes than with strict OOCs of the same length and weight.

B. Extended Prime Codes (EPC)

To reduce the value of λ_c from 2 to 1, each sub-block in the prime code words can be padded with P-1 trailing zeros. These kinds of sequences are called extended prime codes [20]. They have the same code cardinality and weight, but the code length is now increased to $P(2P$-1). Therefore, the EPCs are codes with ($N = P(2P$-1), $W = P$, $\lambda_a = P$-1, $\lambda_c = 1$).

C. Code Comparison

For a given prime number P, the original and extended prime codes have different lengths (i.e. P^2 against $P(2P$-1)). This difference causes extended prime codes to present, for the same data rate B, a reduction in the *chip* time T_c and, consequently, a lower spectral efficiency and, possibly, higher inter-*chip* interference after transmission. On the other hand, as previously said, λ_c is reduced from 2 to 1 in EPCs, which results in a lower MAI.

Consequently, the BER of a EPC, under the restrictions of having the same maximal code length (P^2) and number of simultaneous users K as the original PC, is reduced and EPCs are capable of outperform the original prime sequence [20]. Hence, EPCs sacrifices bandwidth in exchange for better BER performance, even being the weight W lower for a EPC with the same N as a PC.

Although stated in [9] that mode-locked lasers with 16 ps pulses are already commercially available, this kind of laser is costly and its use was avoided. Therefore, in this work a conservative value for the *chip* pulse time duration ($T_c \geq 100$ ps) was used. In addition, data rates of 100 Mbps were simulated for each user (*i.e.* $B = 100$ Mbps). Hence, we have an upper limit for the code length ($N = B_c/B \leq 100$ *chips*).

Using only power of two sequences, the length limit is further reduced ($N \leq 64$ *chips*). As $N = P^2$ for prime codes and $N = P(2P–1)$ for extended prime codes, there is an upper limit of $P \leq 7$ and $P \leq 5$ for PCs and EPCs, respectively. In this work, PCs with $P = 5$ and 7 and an EPC with $P = 5$ were simulated and compared. For comparison purposes, all codes were appended with trailing zeros until being power of two sequences, which keeps the pseudo-orthogonality between codes, as long as the same N is maintained within each family and the delays in each coder are adapted for the new reality.

This further reduces T_c and can represent a worsening in inter-*chip* interference (or inter-symbol interference, caused by dispersion) and synchronization, but represents an improvement in terms of inter-bit interference, caused by decoding. The deconvolution process performed in decoders generates words with $2N$-1 *chips*, which can occupy more *chip* slots than a single bit. Hence, the deconvolution of one bit can interfere in the next bit and the insertion of trailing zeros in each bit represents a time guard, counterattacking this effect.

Brazilian Microwave and Optoelectronics Society-SBMO *received 18 March 2013; for review 24 Apr 2013; accepted 12 July 2013*
Brazilian Society of Electromagnetism-SBMag *ISSN 2179-1074*

This discussion is consolidated in Table I.

TABLE I. CODE COMPARISON

Code Type	Code Length (*N*)	Trailing Zeros	Total Length	Deconvolution Length	Inter-Bit Interference Length	Cross-Correlation Constraint (λ_c)	Weight (*W*)
PC $P = 5$	25 (↑)	7	32 (↑)	49 (↑)	17 (↑)	2 (↓)	5 (↓)
PC $P = 7$	49 (↓)	15	64 (↓)	97 (↓)	33 (↓)	2 (↓)	7 (↑)
EPC $P = 5$	45 (↓)	19	64 (↓)	89 (↓)	25 (-)	1 (↑)	5 (↓)

The symbols ↑, ↓ and – were used to indicate the best, worst and intermediate characteristics, respectively, among all the three codes. The number of trailing zeros was not characterized because they represent a worsening in inter-*chip* interference, but improvement in inter-bit interference.

III. OCDMA-FSO SYSTEM MODEL

The system proposed in this work is based on [1], [9], [16], [21] and is presented in Fig. 1. It was initially thought for multiple users sharing a single FSO channel to transmit coded information. The channel distance is variable, so the transmitter could be installed in a vehicle or any mobile station to communicate with a central base. This system can be an initial step in mobile FSO networks with multiple addressable nodes and multiple channels, if multidirectional FSO links were used.

In the transmission node, the encoded optical signals from all active users are concentrated by an optical coupler before being hard-limited and transmitted. In the reception node, the optical decoders give a high correlation peak to the desired signal before it is detected by the photodetector. The number of simultaneous users may severely limit the user capacity of the system [8]-[9].

In an OCDMA system, although users are not required to be synchronized, it is demonstrated in [15] that *chip* synchronization results in an upper limit on the BER. In addition, the performance of DS systems is extremely dependent on clock recovery. In this work, *chip* synchronization and $\tau_k = 0$ are assumed for all users. The synchronization or clock recovery system is beyond the scope of this work, but some construction methods can be obtained in [16], [22]-[24].

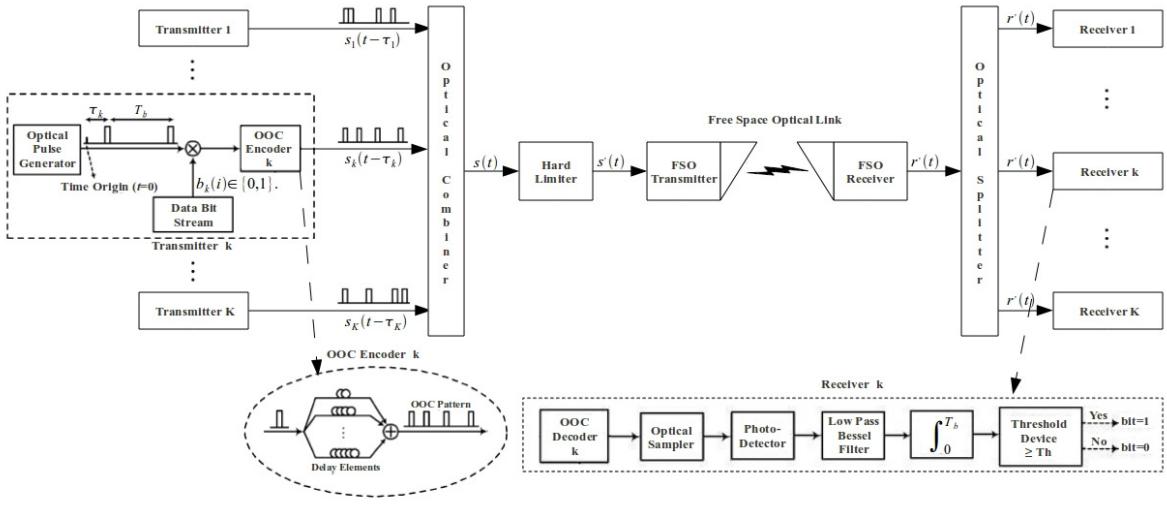

Fig. 1. Basic architecture adopted for the OCDMA-FSO system.

Brazilian Microwave and Optoelectronics Society-SBMO *received 18 March 2013; for review 24 Apr 2013; accepted 12 July 2013*
Brazilian Society of Electromagnetism-SBMag *ISSN 2179-1074*

The whole system was simulated using a commercial tool known as OptiSystem, from Optiwave, Inc. When a desired component was not present in the software or its model was not adequate to our expectations, the device was created using the software MatLab, through an interface component. The simulations were carried out using components as realistic and cost effective as possible.

A. Externally Modulated Optical Transmitter

The subsystem composed by the optical pulse generator and the external modulator present in Fig. 1 was modeled through a continuous wave (CW) laser and a $LiNbO_3$ modulator. So the external modulator was responsible for both shaping the *chips* and inserting the data bit stream.

The carrier wavelength adopted was 1550 nm due to its low attenuation, well suitability for FSO transmission, good eye safety classification and difficulties in beam detection through night-vision scope [4],[25]. The end transmission power was 0 dBm, considering the CW laser transmission power, set to 5 dBm, and the $LiNbO_3$ modulator insertion loss, configured to 5 dB based in [25]-[26].

A parameter that limits the performance of realistic modulators is the extinction ratio (r_{ex}), which is the ability of the device to extinguish the light when it is driven to the bit 0 state [26]-[27]. To simulate the optical $LiNbO_3$ modulator, it was used r_{ex} = 25 dB. This is a high (but usually necessary, for DS systems) extinction ratio, as the system suffers from other signal degradation factors as laser linewidth and carrier phase shift in delay lines. All these effects were considered during simulations. System parameters used in simulations are presented in Table II.

TABLE II. SIMULATION PARAMETERS

Parameter	Value
Laser Wavelength (λ)	1550 nm
Laser Power (P_L)	5 dBm
Laser Linewidth ($\Delta\nu$)	1 MHz
Minimum *Chip* Time ($T_{c,min}$)	156.25 ps
Maximum *Chip* Time ($T_{c,max}$)	312.5 ps
Modulator Insertion Loss (δ_{mod})	5 dB
Modulator Extinction Ratio ($r_{ex,mod}$)	25 dB
Coupler Insertion Loss ($\delta_{coupler}$)	1.3 dB
FSO Transmitter Aperture Diameter (d_T)	5 cm
FSO Transmitter Insertion Loss (α_T)	3 dB
FSO Beam Divergence (θ)	2 mrad
Atmospheric Attenuation (α_{atm})	1 dB/km
Refractive Index Structure Parameter (C_n^2)	10^{-13} $m^{-2/3}$
FSO Receiver Aperture Diameter (d_R)	20 cm
FSO Receiver Insertion Loss (α_R)	3 dB
Optical Sampler Insertion Loss (δ_{sampl})	5 dB
Optical Sampler Extinction Ratio ($r_{ex,sampl}$)	25 dB
APD Multiplication Factor (M)	3
APD Responsivity (ρ)	1 A/W
APD Dark Current (i_d)	10 nA
APD Thermal Noise Power Spectral Density ($S_{thermal}$)	10^{-22} W/Hz
Absolute Temperature (T)	300 K
APD Noise Figure (F_n)	4.57 dB
APD load resistor (R_L)	237.36 Ω
Data Bit Rate (B)	100 Mbps
Number of Samples per Bit (N_s)	512
Number of Transmitted Bits (N_{bits})	1024

Brazilian Microwave and Optoelectronics Society-SBMO *received 18 March 2013; for review 24 Apr 2013; accepted 12 July 2013*
Brazilian Society of Electromagnetism-SBMag *ISSN 2179-1074*

B. DS-OCDMA Encoder

As can be noted from Fig. 1, the DS-OCDMA encoder is composed by a $1 \times W$ splitter, a $W \times 1$ combiner and W optical fibers with different lengths as time delay elements. The first optical fiber can present any length and is responsible for the transmission of the first *chip* ($n = 0$ in (1)), as this *chip* is always set in prime codes. Each one of the other $W - 1$ optical fibers must provide a delay of $n \times T_c$, where n corresponds to 1's position in code.

For simplicity, each fiber was simulated through a single time delay element. Considering the code lengths used in this work ($N = 32$ to 64 *chips*), the time delay difference between optical fibers ranges from 156.25 to 312.5 ps and, thus, the length difference between them varies from ~ 32 to 64 mm. This variation is very small to produce significant loss (typically 0.2 dB/km) or dispersion (typically 16 ps/km·nm) differences between branches and so this simplification can be assumed.

Splitters and combiners are couplers, which were simulated with insertion loss $\delta_{coupler} = 1.3$ dB [28]. This loss can be compensated through branches constructed with erbium-doped fiber amplifiers (EDFAs) [29], which was made in this work.

C. Hard-Limiter

An optical hard-limiter is a threshold element combined with optical feedback to achieve bistability [9], [30]-[32]. It is an important and commonly proposed component for DS-OCDMA applications [25]. An ideal hard-limiter as in [9] and presented in OptiSystem is difficult to be constructed. Hence, this device was programmed in MatLab, in order to achieve a more realistic approximation.

There are two main ways of implementing optical hard-limiters. The first one uses the nonlinear properties of semiconductor optical amplifiers (SOA) [30]-[31]. The other one uses periodic structures consisting of alternating layers of materials possessing different optical Kerr nonlinearity [32]. The non-ideal optical hard-limiter function in this work is based on this last one and is given by:

$$P_{out}(t) = \begin{cases} P_{down}, \, for \; P_{in}(t) < P_{th,down} \\ P_{in}(t), \, for \; P_{th,down} \le P_{in}(t) \le P_{th,up} \\ P_{up}, \, for \; P_{in}(t) > P_{th,up} \end{cases} \tag{5}$$

where P_{down} is the lower output level, P_{up} is the upper output level, $P_{th,down}$ is the lower input power threshold and $P_{th,up}$ is the upper input power threshold. Moreover, it was used: $P_{up} = P_{th,up} = 2 \times P_{th,down}$.

Fig. 2 presents the measured hard-limiter function for five users transmitting in a $K = 5$ system.

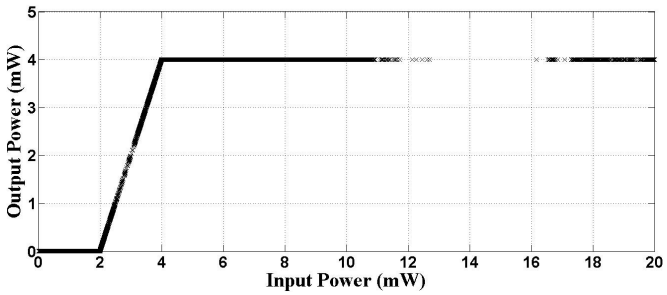

Fig. 2. Input versus output power for the proposed hard-limiter (EPC $P = 5$, $N = 45 + 19 = 64$ and $K = 5$).

Brazilian Microwave and Optoelectronics Society-SBMO *received 18 March 2013; for review 24 Apr 2013; accepted 12 July 2013*
Brazilian Society of Electromagnetism-SBMag *ISSN 2179-1074*

The X-dots show the possible input powers presented by the system. It can be seen, in the point where the power is 4mW, that the proposed hard-limiter only limits the input power, giving no amplification to the signal. The phase from the original signal is kept. An optical hard-limiter has the function of excluding some combinations of interference patterns from becoming heavily localized in a part of signature codes [9]. This way, it attenuates the signal when two or more users transmit a *chip* in the same time slot. The hard-limiter was placed at the transmission end node, because the system is thought for mobile applications and, therefore, the incoming power at the FSO receiver is variable. In the transmission node, when the number of simultaneous users is defined and their power combined, the hard-limiter threshold parameters necessary to eliminate the interference are easier determined.

D. FSO Channel

The FSO channel is a subsystem composed by a transmitter telescope, the free space and a receiver telescope. The propagation distance between transmitter and receiver telescope was set as a variable parameter. The attenuation of the laser power can be calculated through the following equation [4]:

$$P_{r'}(t) = P_{s'}(t)\frac{d_R^2}{(d_T + \theta \cdot L)^2} 10^{-(\alpha_{atm} \cdot L + \alpha_T + \alpha_R + \alpha_{scint})/10} \tag{6}$$

where $P_{r'}(t)$ is the power at the receiver telescope output, $P_{s'}(t)$ is power at the transmitter telescope input, d_R and d_T are, respectively, the receiver and transmitter aperture diameters, θ is the beam divergence, L is the distance, α_{atm} is the atmospheric attenuation, α_{scint} is the loss due to scintillation, α_T and α_R are, respectively, the transmitter and receiver insertion losses due to fiber-telescope interfaces and coupling efficiencies.

One common effect that influences the FSO channel is known as optical turbulence, which is caused by temperature fluctuations manifested as refractive index fluctuations in the atmosphere. This distortion of the wavefront is called scintillation. One way to characterize the turbulence in the channel is by examining the Rytov variance σ_R^2, defined as [33]:

$$\sigma_R^2 = 1.23 \cdot C_n^2 \cdot k^{7/6} \cdot L^{11/6} \tag{7}$$

where $k = 2\pi/\lambda$ is the wave number and C_n^2 is the refractive index structure parameter.

Under weak turbulence conditions, the normalized intensity variance of the optical wave σ_I^2, also called scintillation index, is approximately equal to the Rytov variance, *i.e.* $\sigma_I^2 = \sigma_R^2$ [33]. Hence, the attenuation of the laser power through the atmosphere, due to scintillation, is approximated by [34]:

$$\alpha_{scint} = \exp(\sigma_I) \tag{8}$$

The values chosen for the atmospheric attenuation (α_{atm} = 1 dB/km) and for the refractive index structure parameter ($C_n^2 = 10^{-13}$ m$^{-2/3}$) correspond to a clean weather and to an average scintillation, respectively.

E. DS-OCDMA Decoder with Optical Sampler

As previously said, decoding is performed by intensity correlating the received signal using a matched network of optical delay lines. Therefore, all *chip* pulses from a bit of the same user suffer different delays, so that they are superimposed in the first *chip* slot of the next bit.

Brazilian Microwave and Optoelectronics Society-SBMO *received 18 March 2013; for review 24 Apr 2013; accepted 12 July 2013*
Brazilian Society of Electromagnetism-SBMag *ISSN 2179-1074*

Nevertheless, the optical correlating process generates undesirable temporal side lobes, which result from the other *W*-1 different delays suffered by each *chip* pulse that do not contribute to the correlation peak. In the end, these side lobes contribute to a worsening in the received signal BER, which can turn the system impracticable. To solve this problem, an optical sampler is used. It selects only the main correlation peak and blocks the undesired side lobes.

There are many ways of implementing optical sampling, such as: highly nonlinear fiber (HNLF), nonlinear crystals and waveguides or semiconductor devices [35]-[37]. The simulation approach in this work used another $LiNbO_3$ modulator, placed at the end of the decoder. It leaves only the desired *chip* pulse in the first position of the next bit and gives a small gain. This process has the advantage of also eliminating the cross-correlated pulses resulting from other user. The disadvantages are that it requires another costly modulator and an extremely accurate synchronization system, in order to select only one *chip* slot at a precise position.

F. Photodetector and Integrator

In the proposed system, an avalanche photodiode (APD) was used to convert the optical signal back into electrical form. The total current $i_r(t)$ obtained by the conversion process has the form [1], [25]:

$$i_r(t) = M \cdot \rho \cdot P_r(t) + i_d + i_{thermal} + i_{shot} \tag{9}$$

where the first term represents the current generated by the conversion process and is composed by the APD multiplication factor M, the APD responsivity ρ and the received optical power $P_r(t)$. The second term is the contribution due to dark current i_d and the last two terms are the current fluctuations related to thermal noise $i_{thermal}$ and to shot noise i_{shot}, respectively.

These last two fluctuations are modeled as additive white Gaussian (AWG) noise with double-sided spectral density $S(t)$ [1], [25]:

$$S(t) = \frac{2k_B T F_n}{R_L} + qM^2 F_n(\rho P_r(t) + i_d) \tag{10}$$

where the first term is the thermal noise contribution, formed by the Boltzmann constant k_B, the absolute temperature T, the noise figure of the receiver electronics F_n and the APD load resistor R_L. The second term is the shot noise contribution, where q is the electron charge and the other terms were already defined.

After the optical signal is converted, it passes through an integrator with integration time equal to the bit time T_b and receives a gain of $1/T_b$. As each correlated pulse was placed at the beginning of the next bit, this process makes the pulse last for the entire bit period without losing its original power. Unfortunately, the proposed correlating process imposes a minimum fixed delay of one bit.

G. BER Analysis

Due to memory limitations, the simulations were performed with 1024 bits being transmitted by each user, which is indicated in Table II. Therefore, BER results had to be evaluated using a statistical approach. The BER with an optimum setting of the decision threshold is [25]:

Brazilian Microwave and Optoelectronics Society-SBMO *received 18 March 2013; for review 24 Apr 2013; accepted 12 July 2013*
Brazilian Society of Electromagnetism-SBMag *ISSN 2179-1074*

$$BER = \frac{1}{2} erfc\left(\frac{Q}{\sqrt{2}}\right) \tag{11}$$

where *erfc* stands for the complementary error function and the parameter Q is given by [25]:

$$Q = \frac{I_1 - I_0}{\sigma_1 + \sigma_0} \tag{12}$$

where I_1 and I_0 are the average currents related to bits 1 and 0, respectively, with corresponding variances σ_1^2 and σ_0^2.

This way, when all bits are superimposed to form an eye diagram, one can obtain a punctual BER value, BER(t), calculated from the average currents, $I_1(t)$ and $I_0(t)$, and their variances, $\sigma_1^2(t)$ and $\sigma_0^2(t)$, in a precise bit instant ($0 \leq t < T_b$) within the bit time. Thus, the statistically calculated BER is variable and it has $N_s = 512$ values per user, which is the number of samples per bit shown in Table II.

IV. SIMULATION RESULTS AND DISCUSSION

As said before, the simulations were carried out using components as realistic as possible. This assumption obliged the system to deal with problems, such as extinction ratio in modulators, transmitter laser linewidth and carrier phase shift in delay lines of encoders and decoders. These limiting factors were measured at the combined signal $s(t)$ of all transmitters and are shown in Fig. 3, as an example, where the system was simulated using EPC with $P = 5$.

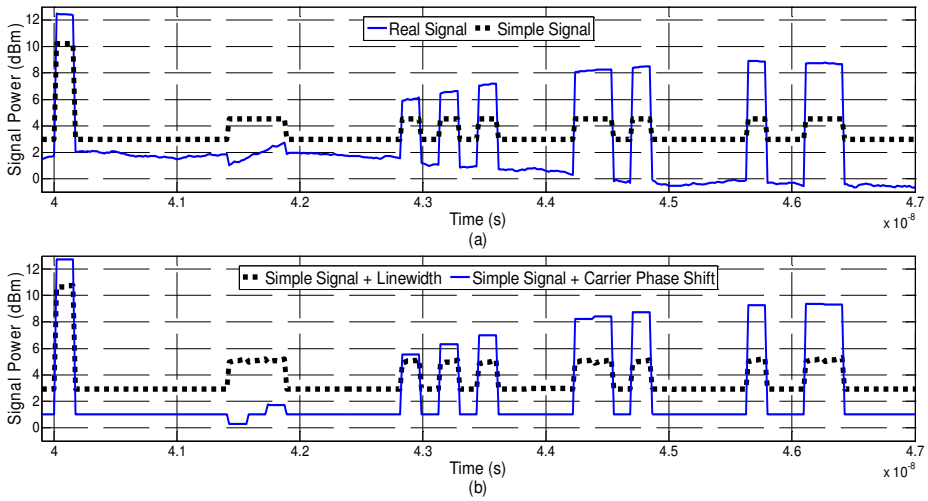

Fig. 3. Influence of extinction ratio, laser linewidth and carrier phase shift in transmitted signal $s(t)$ (EPC $P = 5$, $N = 45 + 19 = 64$ and $K = 5$). (a) Real Signal and Simple Signal. (b) Simple Signal + Linewidth and Simple Signal + Phase Shift.

In Fig. 3, the realistic and simulated signal is identified as "Real Signal". "Simple Signal" is the desired sum of *chips* from different users. "Simple Signal + Linewidth" is the influence of laser linewidth alone and "Simple Signal + Phase Shift" is the influence of carrier phase shift alone.

It can be seen that the linewidth alone produces a small interference in signal amplitude, especially for high level *chips*. The carrier phase shift, though, produces a stronger amplitude variation which, combined with laser linewidth and extinction ratio, generates a strong interference in *chip* levels, especially for level 0. In Fig. 3, the variation for level 0 is greater than 2 dB in one unique bit time.

Brazilian Microwave and Optoelectronics Society-SBMO *received 18 March 2013; for review 24 Apr 2013; accepted 12 July 2013*
Brazilian Society of Electromagnetism-SBMag *ISSN 2179-1074*

Although these values occurred for EPC with $P = 5$, all simulated codes presented such variations.

This strong interference must be handled by the optical hard-limiter in the transmitter output through careful choice of its input threshold parameters. The parameters were configured in order to give minimum BER for each one of the transmitting users. Hence, in addition to excluding the occurrence of two or more *chips* in the same time slot, the hard-limiter was also used to control the interference effects shown in Fig. 3. With this purpose, the lower input threshold $P_{th,down}$ was defined about 10% above level 0 average power, thus, equalizing this level as long as the interference was not too high. In the same way, $P_{th,up}$ was used to equalize level 1 *chips*.

Starting the simulations, the extended prime code with $P = 5$ was the first kind of code that was tested, because of its predicted smaller MAI in comparison with prime sequences with near the same length. This code allows a maximum of five simultaneous transmitting users, when not using its shifted versions. As previously said, the simulations were carried out varying the FSO channel distance. The measured BER at the receiver output for each user is presented in Fig. 4.

It can be seen that the worst BER (considering five different 1024 bits sequences used for each transmitter) was achieved by user coded with the 5th EPC. Even so, this user achieved a BER $\leq 10^{-9}$ for distances up to 1.2 km, demonstrating its functionality for up to five users with good link quality.

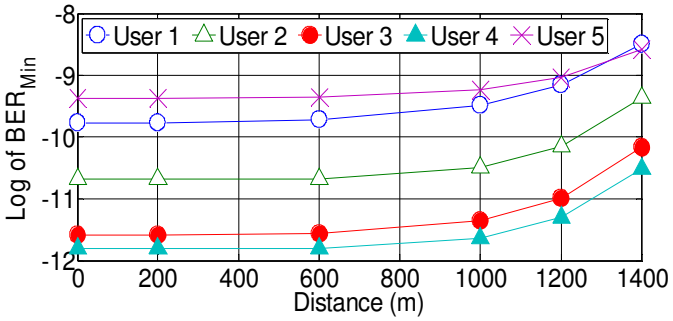

Fig. 4. Minimum BER for five users (EPC $P = 5$, $N = 45 + 19 = 64$ and $K = 5$).

Other considerations should be taken at this moment. These BER results consider all the effects previously discussed, such as extinction ratio in modulators, transmitter laser linewidth, carrier phase shift in delay lines, along with thermal, shot and dark current noises in photodetector, which were calculated using Table II.

Furthermore, in order to guarantee the statistical behavior of simulations, the data bit stream for each user was generated through a pseudo-random algorithm with different random seed index for each user. Therefore, the fact that only 1024 bit sequences were generated, combined with the inter-bit interference, explained in subsection II.C, turns the BER more susceptible to the bit patterns being transmitted by each user and is perceived in the different BER results in Fig. 4. Despite these differences, the worst case analysis guarantees the system functionality for the used code family.

In addition, the results present the minimum achieved BER in a bit period. This minimum BER normally does not last for the entire bit period, which forces the system to have a well synchronized threshold detector in order to sustain the minimum BER for that user. This feature is seen in Fig. 5.

Brazilian Microwave and Optoelectronics Society-SBMO *received 18 March 2013; for review 24 Apr 2013; accepted 12 July 2013*
Brazilian Society of Electromagnetism-SBMag *ISSN 2179-1074*

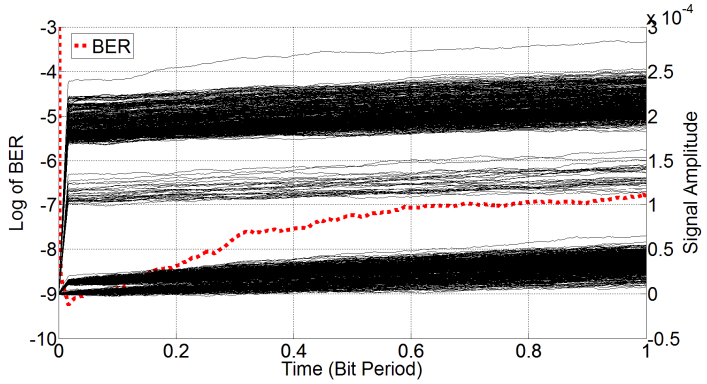

Fig. 5. Eye diagram for 1024 bits and instantaneous BER for user 5 and L = 1 km (EPC P = 5, N = 45 + 19 = 64 and K = 5).

Hence, although a good eye opening is presented, the BER of 10^{-9}, commonly required for optical communication systems, is achieved only in a small fraction of time. If the detection instant is badly predicted, the BER obtained for this user would be higher than expected.

Besides, Fig. 3 shows that some *chips*, after suffering from interference, present power amplitude below the noisy low level. Consequently, they are interpreted by the hard-limiter as low level *chips* and are lost in the codification. This effect can be observed in Fig. 5. The intermediate amplitude levels represent *chips* that were lost in codification of some bits. Therefore, the decoder receives fewer *chips* to sum and the integrator achieves these intermediate levels.

Taking these facts into consideration, two other codes were implemented: PC with P = 5 and 7. Although prime code systems with P = 7 should allow up to seven code words (users), the proposed system achieved again a maximum of five simultaneous users. When testing the system for six or seven simultaneous users, the MAI with the realistic considerations made before was so high, that some of them presented BER results worse than 10^{-9}, which was undesirable. Fig. 6 presents the BER results for four of six simultaneous transmitting users using P = 7 PC. The results for the other two users (4 and 5) are not shown because they presented BER < 10^{-15}. It is shown that the result for user 1 is not acceptable, since its BER > 10^{-9} for any distance. Hence, the system is also limited to five users, when using this kind of code, and all the simulated codes achieved a maximum aggregated bit rate of 500 Mbps, when all five users were transmitting simultaneously.

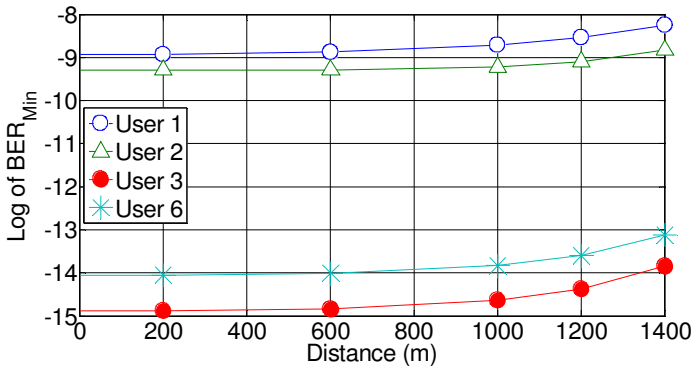

Fig. 6. Minimum BER for four of six users (PC P = 7, N = 49 + 15 = 64 and K = 6).

Brazilian Microwave and Optoelectronics Society-SBMO *received 18 March 2013; for review 24 Apr 2013; accepted 12 July 2013*
Brazilian Society of Electromagnetism-SBMag *ISSN 2179-1074*

At this point, all the three kind of code systems (PC with $P = 5$, PC with $P = 7$ and EPC with $P = 5$) were simulated for $K = 3$ to 5 simultaneous users and the minimum BER results were compared. In order to perform this comparison, the worst case minimum BER of all K simulated users was selected to characterize the code influence upon the system. This comparison is performed in Fig. 7. It can be observed that best BER results were achieved by the PC with $P = 7$ for $K = 5$ simultaneous transmitting users, while for $K = 4$ and 3, the best results were for PC with $P = 5$.

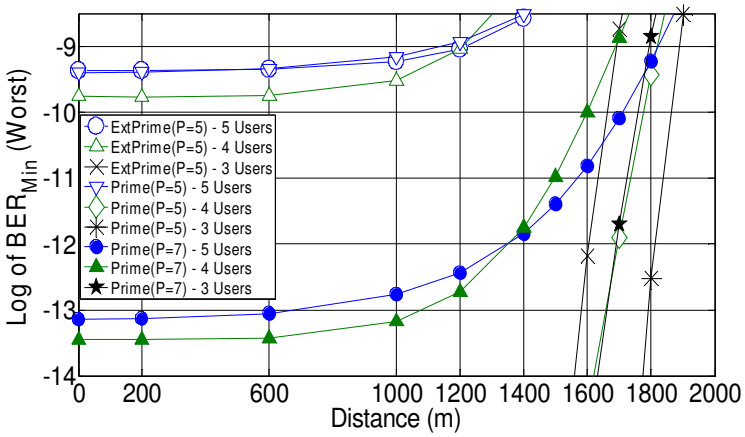

Fig. 7. Worst case minimum BER for different codes ($K = 3$ to 5).

Fig. 7 also shows that some systems with smaller number of users present worst BER after long distances. This can be explained by the hard-limiter effect. With fewer users, the noisy low level at the combined signal $s(t)$ of all transmitters (*chip* level 0) observed in Fig. 3 becomes lower. Having in mind that $P_{th,down}$ was defined about 10% above level 0 average power, the threshold parameter of the hard-limiter has to be changed to lower levels in order to keep good BER results for these systems. As a compromise, in systems with fewer users, BER is improved in exchange for power. This lower power strongly influences the BER after long distances, when the results become worse. As a result, the proposed hard-limited system must keep control of the number of simultaneously transmitting users, in order to adjust its threshold parameters to achieve lower BER. If it was not performed, the system would achieve worst BER results in general for fewer users, what is not desirable.

It is also observed that, unlike predicted when analyzing only the cross-correlation constraint in λ_c Table I, the worst BER results were obtained by using extended prime codes. This result is due to the hard-limiter at the transmitter, associated with optical sampler at the receiver, which already provided the BER improvement that would be achieved by EPC. These devices help to eliminate the undesired side lobes and have a stronger impact in reducing λ_c for the PCs ($\lambda_c = 2$) than for the EPC ($\lambda_c = 1$). Therefore, two factors played a very important role in BER improvement: the longer *chip* time of PC with $P = 5$ (32 *chips* per code) and the higher number of *chips* of PC with $P = 7$. When the system had to face a higher MAI ($K = 5$), the higher autocorrelation peak of PC with $P = 7$ was preponderant, while for a lower MAI ($K = 3$ or 4), a shorter and simpler code (PC $P = 5$) was more important.

As previously said, the BER results presented up to now can lead to misinterpretation, because they represent the minimum achieved value in a bit period. A code with worse minimum BER (but still ≤

10^{-9}) could sustain this BER for a longer period of time and would relieve the threshold detector, representing a better system performance. Therefore, the period of time for which the BER was kept bellow 10^{-9} was calculated for each type of code. Again, the results are presented for the user with worst BER performance in Fig. 8. It can be seen that the best time results were obtained again by PC with $P = 7$ for $K = 5$, while for $K = 4$ and 3, the best results were for PC with $P = 5$. These systems kept BER $\leq 10^{-9}$ for almost the entire bit period ($T_b = 10^{-8}$ s) for up to 1 km.

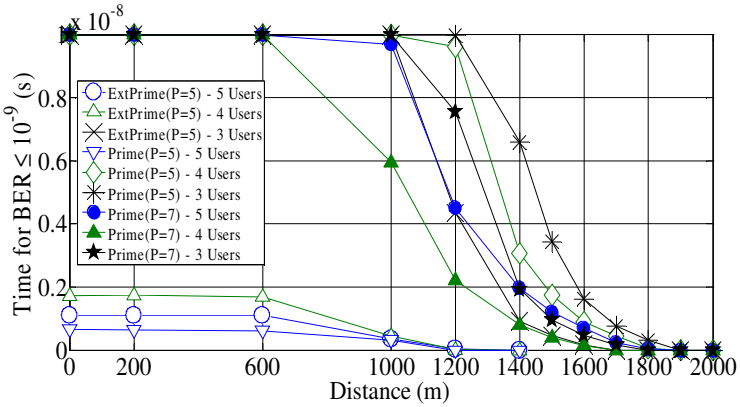

Fig. 8. Period of bit time for BER $\leq 10^{-9}$ for different codes ($K = 3$ to 5).

In order to gain a perspective of the received power influence upon the BER results presented in Fig. 7 and 8, a figure of merit is shown in Fig. 9. The codes analyzed were PC with $P = 7$ for $K = 5$, PC with $P = 5$, for $K = 4$ and 3, which were the ones that presented best BER performance, and EPC with $P = 5$, for $K = 3$, which presented best performance among all EPC. The power shown in Fig. 9 is the electrical average power at the receiver output for the worst case user and corresponds to distances between 1.5 and 2 km.

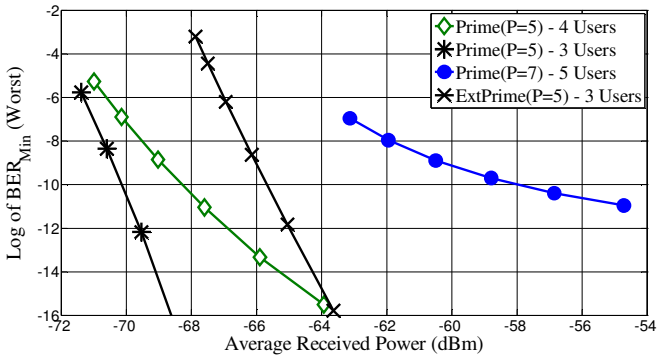

Fig. 9. Worst case minimum BER as a function of the average received power ($K = 3$ to 5, $L = 1{,}5$ to 2 km and $N_{bits} = 256$).

It can be seen that, as the number of users grows, the system requires a higher power on average to maintain the same BER level. This is in agreement with the previously said about a higher threshold level being necessary in the hard-limiter stage, because more users (higher power) are being combined in its input. It can also be observed that the EPC required, on average, about 4 dB more power than its PC counterpart to achieve the same BER levels, although the same input threshold parameters were used for both cases.

Brazilian Microwave and Optoelectronics Society-SBMO *received 18 March 2013; for review 24 Apr 2013; accepted 12 July 2013*
Brazilian Society of Electromagnetism-SBMag *ISSN 2179-1074*

Finally, in order to evaluate the impacts of FSO channel on the OCDMA communication system and how the beam spreading affects the system functionality, the divergence angle was changed and the system was simulated for a distance of 1.2 km. The codes analyzed were PC with $P = 7$ for $K = 5$ and PC with $P = 5$, for $K = 4$ and 3, which were the ones that presented best BER performance. The results are presented for the user with worst BER performance in Fig. 10.

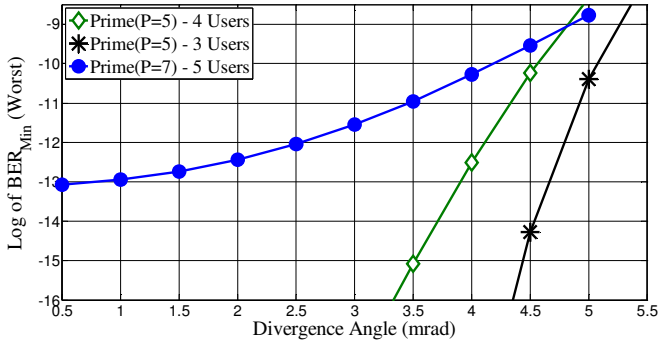

Fig. 10. Worst case minimum BER for different divergence angles ($K = 3$ to 5 and $L = 1.2$ km).

It can be noted that, for this distance, the system supports divergence angles up to 4.8 mrad for all kinds of codes and number of users. Hence, the OCDMA system proposed in this work can have a very spread beam, being less susceptible to misalignment problems, which means it can have a simpler tracking system. In addition, although the system can more easily suffer interceptions, as previously discussed, the signal is still encoded and difficult to be understood.

V. CONCLUSION

The results demonstrate the capacity and functionality of the proposed OCDMA-FSO system. Although some devices need a lower cost design, such as hard-limiters and optical samplers, all components were simulated as realistic and cost-effective as possible.

This work took into account the effects of extinction ratio in modulators, transmitter laser linewidth and carrier phase shift in delay lines of encoders and decoders, along with thermal, shot and dark current noises in photodetector. It was demonstrated that the previous effects impose a precise control of power amplitude in the hard-limiter in order to keep good BER results. Signal distortions of above 2 dB were demonstrated.

It was shown that the system supported a maximum of five simultaneous transmitting users, for the proposed configuration, code lengths, data rate, distances and divergence angles. The proposed system can be extended in the future to mobile FSO networks with multiple addressable nodes and multiple channels, if multidirectional FSO links were used.

A maximum combined bit rate of $B = 5$ (users) × 100 Mbps = 500 Mbps was achieved by the system. The results show that each user achieved BER under 10^{-9} for every code tested for distances up to 1.2 km and divergence angles of 2 mrad. They also show that each user presents better BER results, when the MAI influence is reduced ($K = 4$ and 3 users). Nevertheless, only some kinds of

Brazilian Microwave and Optoelectronics Society-SBMO *received 18 March 2013; for review 24 Apr 2013; accepted 12 July 2013*
Brazilian Society of Electromagnetism-SBMag *ISSN 2179-1074*

codes sustain these maximum BER results for more than 50% of the bit time.

Therefore, when maximum and fully multiplexed bit rate is needed, *i.e.*, five users, the results suggest as direct sequence the use of prime codes with $P = 7$ for distances up to 1.2 km and divergence angles up to 2 mrad. For fewer users (or lower bandwidth), it is suggested the use of PC with $P = 5$ for distances up to 1.4 km, in order to keep a good threshold detection time period.

In addition, it was observed that the system supports divergence angles up to 4.8 mrad for distances up to 1.2 km. Hence, if a well synchronized threshold detection device is used, the OCDMA-FSO system proposed in this work can be less susceptible to misalignment problems, which means having a simpler tracking system.

ACKNOWLEDGMENT

The authors would like to thank CNPq (Conselho Nacional de Desenvolvimento Científico e Tecnológico) and the Brazilian Army for partially supporting this work.

REFERENCES

[1] A. Bekkali, P. T. Dat, K. Kazaura, K. Wakamori and M. Matsumoto, "Performance Analysis of SCM-FSO Links for Transmission of CDMA Signals under Gamma-Gamma Turbulent Channel," Military Communications Conference, 2009, MILCOM 2009, IEEE, pp. 1-5.

[2] V. W. S. Chan, "Free-Space Optical Communications," Journal of Lightwave Technology, vol. 24, no. 12, pp. 4750-4762, Dec 2006.

[3] D. M. Forin, G. Incerti; G. M. T. Beleffi ; A. L. J. Teixeira, L. N. Costa, P. S. B. André, B. Geiger, E. Leitgeb and F Nadeem, "Free Space Optical Technologies," in Trends in Telecommunications Technologies, C. J Bouras, Ed. Vukovar, Croatia: In-Tech, 2010, pp. 257–296.

[4] S. Bloom, E. Korevaar, J. Schuster and H. Willebrand, "Understanding the performance of free-space optics," Journal of Optical Networking, vol.2, no. 6, pp. 178–200, Jun 2003.

[5] B. Barua and S. P. Majunder, "Performance Analysis of an LDPC Coded FSO Communication System with Different Modulation Technique under Turbulent Condition," 15th International Conference on Computer and Information Technology (ICCIT 2012), pp. 240-243, Dec 2012.

[6] B. Patnaik and P. K. Sahu, "Novel QPSK Modulation for DWDM Free Space Optical Communication System," Wireless Advanced (WiAd 2012), pp. 170-175, Jun 2012.

[7] E. Ciaramella, Y. Arimoto, G. Contestabile, M. Presi, A. D. Errico, V. Guarino, and M. Matsumoto, "1.28 Terabit/s (32x40 Gbit/s) WDM Transmission System for Free Space Optical Communications," IEEE Journal on Selected Areas in Communications, vol. 27, no. 9, pp. 1639-1645, Dec 2009.

[8] N. G. Tarhuni, "Fiber-Optic Code Division Multiple Access: Multi-Class Optical Orthogonal Codes, Optical Power Control and Polarization Encoding," Ph.D. dissertation, Dept. Elect. Comm. Eng., Helsinki Univ. of Technology, Espoo, Finland, 2007.

[9] J.-J. Chen and G.-C. Yang, "CDMA Fiber-Optic Systems with Optical Hard Limiters," Journal of Lightwave Technology, vol. 19, no. 7, pp. 950-958, Jul 2001.

[10] P. R. Prucnal, M. A. Santoro and T. R. Fan, "Spread Spectrum Fiber-Optic Local Area Network Using Optical Processing," Journal of Lightwave Technology, vol. 4, no. 5, pp. 547-554, May 1986.

[11] V. J. Hernandez, W. Cong, J.Hu, C. Yang,N.K. Fontaine, R. P. Scott, Z. Ding, B. H. Kolner, J. P. Heritage, and S. J. B. Yoo, "A 320-Gb/s Capacity (32-User × 10 Gb/s) SPECTS O-CDMA Network Testbed With Enhanced Spectral Efficiency Through Forward Error Correction," Journal of Lightwave Technology, vol. 25, no. 1, pp. 79–86, Jan. 2007.

[12] P. L. L. Bertarini, A. L. Sanches, and Ben-Hur V. Borges, "Optimal Code Set Selection and Security Issues in Spectral Phase-Encoded Time Spreading (SPECTS) OCDMA Systems," Journal of Lightwave Technology, vol. 30, no. 12, Jun 2012.

[13] F. R. K. Chung, J. A. Salehi and V. K. Wei, "Optical Orthogonal Codes: Design, Analysis, and Applications," IEEE Transactions on Information Theory, vol. 35, no. 3, pp. 595-604, May 1989.

[14] J. A. Salehi, "Code Division Multiple-Access Techniques in Optical Fiber Networks-Part I: Fundamental Principles," IEEE Transactions on Communications, vol. 37, no. 8, pp. 824-833, Aug 1989.

[15] J. A. Salehi and C. A. Brackett, "Code Division Multiple-Access Techniques in Optical Fiber Networks-Part II: Systems Performance Analysis," IEEE Transactions on Communications, vol. 37, no. 8, pp. 834-842, Aug 1989.

[16] A. Keshavarzian and J. A. Salehi, "Multiple-Shift Code Acquisition of Optical Orthogonal Codes in Optical CDMA Systems," IEEE Transactions on Communications, vol. 53, no. 4, pp. 687-697, Apr 2005.

[17] A. A. Shaar and P. A. Davies, "Prime Sequences: Quasi-Optimal Sequences for OR Channel Code Division Multiplexing," Electronic Letters, vol. 19, no. 21, pp. 888-890, Oct 1983.

received 18 March 2013; for review 24 Apr 2013; accepted 12 July 2013

ISSN 2179-1074

[18] W.C. Kwong, P.A. Perrier and P.R. Prucnal, "Performance Comparison of Asynchronous and Synchronous Code-Division Multiple-Access Techniques for Fiber-optic Local Area Networks," IEEE Transactions on Communications, vol. 39, no. 11, pp.1625-1634, Nov 1991.
[19] J.-G. Zhang and G. Picchi, "Tunable Prime-Code Encoder/Decoder for All-Optical CDMA Applications," Electronic Letters, vol. 29, no. 13, pp. 1211-1212, Jun 1993.
[20] G.-C. Yang and W.C. Kwong, "Performance Analysis of Optical CDMA with Prime Codes," Electronic Letters, vol. 31, no. 7, pp. 569-570, Mar 1995.
[21] S. Zahedi and J. A. Salehi, "Analytical Comparison of Various Fiber-Optic CDMA Receiver Structures," Journal of Lightwave Technology, vol. 18, no. 12, pp. 1718-1727, Dec 2000.
[22] B. M. Ghaffari, M. D. Matinfar and J. A. Salehi, "Wireless Optical CDMA LAN: Digital Implementation Analysis," IEEE Journal on Selected Areas in Communications, vol. 27, no. 9, pp. 1676-1686, Dec 2009.
[23] Z. Hu, H.-F. Chou, K. Nishimura, M. Usami, J. E. Bowers and D. J. Blumenthal, "Optical Clock Recovery Circuits Using Traveling-Wave Electroabsorption Modulator-Based Ring Oscillators for 3R Regeneration," IEEE Journal of Selected Topics in Quantum Electronics, vol. 11, no. 2, pp. 329-337, Mar/Apr 2005.
[24] V. Roncin, S. Lobo, M.-N. Ngo, L. Bramerie, A. O'Hare, M. Joindot and J.-C. Simon, "Patterning Effects in All-Optical Clock Recovery: Novel Analysis Using a Clock Remodulation Technique," IEEE Journal of Selected Topics in Quantum Electronics, vol. 16, no. 5, pp. 1495-1502, Sep/Oct 2010.
[25] G. P. Agrawal, Fiber-Optic Communication Systems. 3rd ed. New York: John Wiley & Sons, 2002.
[26] M. M. Howerton, R. P. Moeller, A. S. Greenblatt, and R. Krähenbühl, "Fully Packaged, Broad-Band LiNbO3 Modulator with Low Drive Voltage," IEEE Photonics Technology Letters, vol. 12, no. 7, pp. 792-794,Jul 2000.
[27] E. L. Wooten, K. M. Kissa, A. Yi-Yan, E. J. Murphy, D. A. Lafaw, P. F. Hallemeier, D. Maack, D. V. Attanasio, D. J. Fritz, G. J. McBrien and D. E. Bossi, "A Review of Lithium Niobate Modulators for Fiber-Optic Communications Systems," IEEE Journal of Selected Topics in Quantum Electronics, vol. 6, no. 1, pp. 69-82, Feb 2000.
[28] P. D. Trinh, S. Yegnanarayanan, and B. Jalali, "5 x 9 Integrated Optical Star Coupler in Silicon-on-Insulator Technology," IEEE Photonics Technology Letters, vol. 8, no. 6, pp. 794-796, Jun 1996.
[29] H. M. Presby and C. R. Giles, "Amplified Integrated Star Couplers with Zero Loss," IEEE Photonics Technology Letters, vol. 3, no. 8, pp. 724-726, Aug 1991.
[30] G. T. Kanellos, N. Pleros, C. Bintjas, H. Avramopoulos, and G. Guekos, "SOA-based interferometric optical hard-limiter," in Optical Amplifiers and Their Applications/Integrated Photonics Research, Technical Digest (CD) (Optical Society of America, 2004), paper JWB8.
[31] X. Wu, K. Qiu and Y. Ling, "Novel optical power equalizer and optical hard limiter based on quantum-dot semiconductor optical amplifiers", Proc. SPIE 7135, 71353N (2008).
[32] L. Brzozowski and E. H. (T.) Sargent, "All-Optical Analog-to-Digital Converters, Hardlimiters, and Logic Gates," Journal of Lightwave Technology, vol. 19, no. 1, pp. 114-119, Jan 2001.
[33] S. Trisno, "Design and Analysis of Advanced Free Space Optical Communication Systems," Ph.D. dissertation, Dept. Elect. Comp. Eng., University of Maryland, 2006.
[34] T. V. N. Coelho, "Estudo de Sistemas de Comunicação Utlizando Óptica no Espaço Livre," M.S. Thesis in Portuguese, Dept. Electr. Eng., Instituto Militar de Engenharia, Rio de Janeiro, Brazil, 2008.
[35] G. Berrettini, A. Bogoni, F. Fresi, G. Meloni and L. Potì, " Evolution of Optical Sampling," in Advances in Lasers and Electro Optics," N. Costa and A. Cartaxo, Ed. Vukovar, Croatia: In-Tech, 2010, pp. 289–314.
[36] A. Bogoni, F. Ponzini, M. Scaffardi, P. Ghelfi, and L. Potì, "New Optical Sampler Based on TOAD and Data Postprocessing for Subpicosecond Pulse Resolution," IEEE Journal of Selected Topics in Quantum Electronics, vol. 10, no. 1, pp. 186-191, Jan/Feb 2004.
[37] M. Maruyama, K. Uekusa, T. Konno, N. Sato, M. Kawabata, T. Hato, H. Suzuki, and K. Tanabe, "HTS Sampler With Optical Signal Input," IEEE Transactions on Applied Superconductivity, vol. 17, no. 2, pp. 573-576, Jun 2007.

Brazilian Microwave and Optoelectronics Society-SBMO *received 18 March 2013; for review 24 Apr 2013; accepted 12 July 2013*
Brazilian Society of Electromagnetism-SBMag *ISSN 2179-1074*